Desalination and Water Treatment
www.deswater.com
doi: 10.5004/dwt.2020.25313

187 (2020) 163–171
May

Storm water management in country parks in complex orogenic belts

Bohang Sun[a,b], Yan Liu[a,*]

[a]*School of Architecture, Tianjin University, Tianjin 300000, China, email: yogurt61@126.com (Y. Liu)*
[b]*Art Department, Tangshan University, Tangshan 063000, China*

Received 10 June 2019; Accepted 19 December 2019

ABSTRACT

In the case of heavy rain in the complex orogenic belts, to solve the heavy load on the drainage network and the guilt of the country park, the stormwater management model (SWMM) is combined with the low impact development (LID) module to design stormwater management methods. A country park in complex orogenic belts in the south of J City is used as a research area, and the stormwater management model is established according to the current situation of the study area. The operational parameters of the stormwater model in the study area are determined by the sub-catchment generalization, the runoff calculation model, and the confluence calculation model. After the model is verified, when the design return period is 1a, 3a, 5a, 10a, 20a, the SWMM model is used to simulate the total rainwater discharge, drain flow and rainfall-runoff in the study area before and after the LID facility is implemented. The results show that the stormwater management method can accurately simulate the surface runoff in different return periods, which can also reduce rainfall runoff and alleviate the pressure of the drainage network. The total amount of water storage in the study area is 23,742 m^3, which is conducive to alleviating flooding in the complex orogenic belts.

Keywords: Complex orogenic belts; Country park; Stormwater management; SWMM model; LID

1. Introduction

In complex orogenic belts, there are a variety of landform types. These include the braided complex orogenic belts, such as suture structures, truss-architectures, inter-mountain areas, complex barrier combinations, structural steps, and large inter-mountain basins [1]. A large number of plants are distributed on complex orogenic belts, which have inevitable natural functions in limiting urban infinite expansion, rainwater savings management, and strengthening ecological green space. There are many advantages to building a country park in the complex orogeny. On the one hand, it provides a relaxing and enjoyable outing environment for urban people and brings people a natural outing experience; on the other hand, it contributes to preventing desertification and increasing mountain use rate [2]. With the acceleration of urbanization, the artificial paving rate of the interior of the city is getting higher and higher, the area of green space is getting smaller and smaller, and a lot of natural rainwater is wasted, not recycled. People pay more attention to stormwater management in the city, and there is little attention to stormwater management in country parks in complex orogenic belts [3].

At present, stormwater management technology is increasingly strengthened, and the development trend is diversified. Each country has summarized rainwater management technologies suitable for their respective national conditions. For example, stormwater management in the United States is mainly to improve the penetration of nature. It emphasizes that stormwater management combines with natural conditions such as vegetation, water bodies and green spaces to join the artistic aspects of the landscape. British rainwater technology pays more attention to the management of rainwater and the combination of ecology and landscape design, which is more stable and comprehensive. At the heart of Australia's stormwater management is the inclusion of facilities in landscape design to provide a variety of functional spaces, such as animal and plant habitats, public open spaces,

* Corresponding author.

and recreational facilities and visual enjoyment. In China, the development of rainwater management started relatively late, and it is still in the development stage. It mainly implements the stormwater management of the city from the perspectives of environmental engineering, green space planning, municipal administration and special planning. It pays more attention to the standards of planning, the determination of sensitive areas, the analysis of hydrology and the rationalization of rainwater storage of different substrates.

Based on the technology of stormwater management in various countries, the storm water management model (SWMM) is the earliest developed and currently the most widely used urban stormwater management model [4]. Today, SWMM has been widely used in the simulation, analysis and design of urban stormwater runoff, drainage piping systems, watershed planning, etc., and is gradually being applied in non-urban areas [5]. The low impact development (LID) module in the SWMM model mainly reduces the flow of urban stormwater runoff through stagnation, sedimentation, biosorption, infiltration, filtration, and microbial degradation. Eventually, the runoff generation time is delayed, the flood peak is reduced, and the pollutant load on the downstream area is reduced. LID is a series of measures scattered throughout the region to regulate rainfall runoff from the source. Also, it can incorporate land landscapes with self-runoff control capabilities such as gentle slopes and intercepting depressions into the entire rainwater control system [6]. LID's optimization program provides decision-making reference for the control of stormwater management in country parks in complex orogenic belts. To this end, this paper combines SWMM and LID to comprehensively manage the rain and flood conditions in country parks in the complex orogenic area. In the end, we will design the reasonable water-melting facility to enhance the water storage capacity of the country parks, and avoid floods and pollution of surface runoff.

2. Materials and methods

2.1. Overview of the study area

2.1.1. Location analysis

A country park in complex orogenic belts in the south of J City is used as a research area. The research area covers an area of 174 hectares. It is bounded by Langmao Mountain in the north, South second elevated road in the south, and a north mountain of Mafengzhai, Mawuzhai and Shifangyu in the west. Most of the surrounding areas are residential areas with convenient transportation and a good natural environment.

2.1.2. Analysis of the status quo

2.1.2.1. Topography and landform The terrain of the study area is high in the northwest and low in the southeast. In the hilly area, the highest point of the area is 296 m above sea level. The park terrain is high in the southeast and low in the northwest. From the perspective of the current park matrix, most of it penetrates in the form of nature, and there are some residual plants in the northeast and southwest. According to the nature of the existing site, most of them belong to the exposed surface. The soil of the park is the old red sandstone of the Lagrange mudstone series. The soil properties are slightly acidic red loam [7–9]. Generally, the sedimentary mudstone has a high porosity of 60%–70%, and the sedimentary sandstone should have a porosity of 30%–40%.

2.1.2.2. Climate Because the study area is located in the mid-latitude zone, it is affected by solar radiation, atmospheric circulation and geographical environment, and belongs to the warm temperate semi-humid monsoon climate. Affected by the Siberian monsoon, it formed a continental monsoon climate with hot summers and cold winters (four distinct seasons). The annual average temperature in the study area is 14.7°C, the monthly average temperature in January is –0.4°C, and the monthly average temperature in July is 27.5°C. The monsoon climate in the study area is remarkable. The climate in the four seasons is mainly windy and dry in spring, hot and rainy in summer, cool in autumn, and long in dry and cold in winter. The average annual rainfall in the study area is 1,079–1,159 mm. The annual rainfall is unevenly distributed and the summer is the most, accounting for 42% of the total annual precipitation. The annual evaporation is mostly 1,000–1,300 mm, which is roughly equal to or slightly greater than the annual rainfall [10].

2.1.2.3. Advantages Natural conditions: (1) The rainfall is rich and has a good space for rainwater management technology design. The terrain has a clear slope, which is beneficial to the direct collection of rainwater and avoids more manpower construction. (2) Most of the park's ground is a natural way of infiltration, which provides superior conditions for the natural penetration of rainwater.

2.1.2.4. Disadvantages The park matrix was extensively damaged, leaving only a small part of the vegetation and abandoned sites abandoned by the quarry. The plants were reduced and destroyed, the soil became stronger and the penetration of rainwater became worse. Therefore, soil erosion is prevented in areas with dense contours. The advantage of terrain with height differences also poses certain challenges [11]. The storage of rainwater is determined by the slope of the terrain, so attention should be paid to some terrain and area issues in areas where rainwater harvesting is selected.

2.2. Construction of the SWMM

2.2.1. Overview and structure of the model

SWMM is a rainfall-runoff model based on a single event or long-term precipitation sequence. It is mainly used for dynamic simulation of rainfall-runoff water quality and water quality in urban areas. It can edit the data input in the study area, simulate hydrology, hydraulics, water quality, and display the results in various forms, including time-series and charts, profiles and statistical frequency analysis [12]. The SWMM model is mainly composed of a computing module and a service module, as shown in Fig. 1. The calculation module includes the runoff, the conveying, the extended conveying, the storage/processing module; and the service module includes the statistics, the chart, the joint rainfall, and the temperature module.

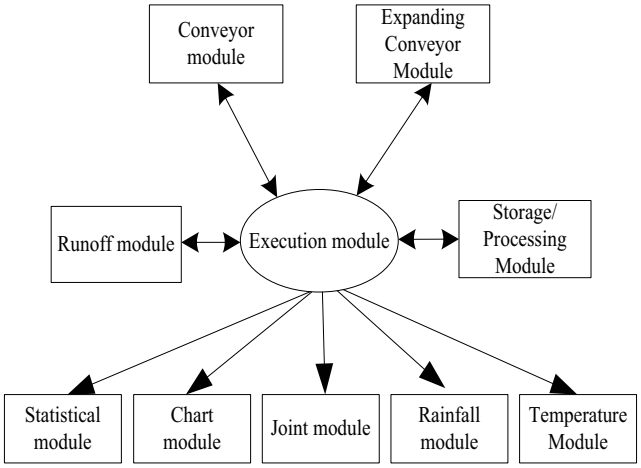

Fig. 1. Structural schematic of the SWMM model.

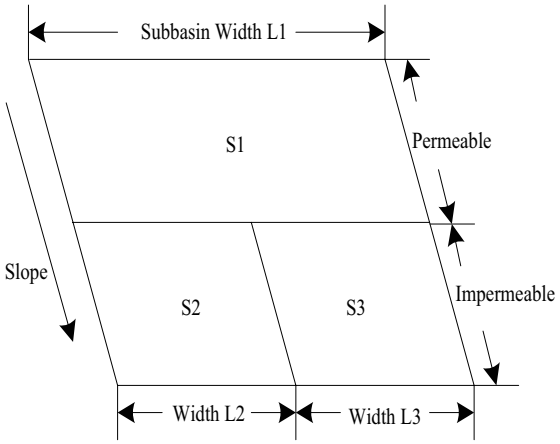

Fig. 2. Summary of catchment watershed.

2.2.2. Generalization of sub-catchment area

The sub-catchment area is a hydrological response unit. On the topography, the surface runoff and drainage system of a sub-catchment have only one water outflow [13,14]. In the SWMM model, it is first necessary to divide the studied catchment area into a series of sub-catchments. Then calculate the respective runoff processes according to the characteristics of each sub-catchment. Finally, the flow calculus method is used to summarize the outflows of each sub-catchment area [15].

As shown in Fig. 2, the catchment sub-basin is divided into a water-permeable area and a water-impermeable area. *S*1 represents the storage area and the water-permeable area, *S*2 represents the storage area and the water-impermeable area, and *S*3 represents the storage area without water storage. *L*1 is both the width of the entire sink sub-basin and the width of *S*1, *L*2, and *L*3 are the widths of *S*2 and *S*3, respectively. The correlation between the three is shown in Eq. (1):

$$L_2 = \frac{S_2}{S_2 + S_3} \times L_1; L_3 = \frac{S_3}{S_2 + S_3} \times L_1 \tag{1}$$

2.2.3. Computation model of runoff generation

Surface runoff refers to the process of rain loss minus loss becoming net rain. In the SWMM model, the runoff of the above three types of surface is calculated separately, and then the runoff process line of the catchment sub-basin is obtained by weighted averaging the area of the three types of the surface [16].

- In the impermeable area, a small part of the rainfall is converted into evaporation, and most of the remaining are converted into a runoff. Runoff is formed when rainfall is greater than evaporation [17]. The calculation of runoff generation is shown in Eq. (2):

$$R_1 = P - E \tag{2}$$

where, R_1 means runoff generation without water storage area, the unit is mm; *P* means rainfall, the unit is mm; *E* is the evaporation amount, the unit is mm.

- In areas with sloping and impervious areas, rainfall begins to form runoff after meeting the maximum turbulence on the ground. The calculation of runoff generation is shown in Eq. (3):

$$R_2 = P - D \tag{3}$$

where, R_2 indicates the runoff generation of the impounded and impervious area, the unit is mm; *P* indicates the rainfall, the unit is mm; *D* indicates the maximum turbulence of the ground, the unit is mm.

- In the permeable area, rainfall first meets surface infiltration requirements. When the rainfall intensity is greater than the infiltration intensity, the ground begins to accumulate water; until the maximum turbulence of the ground reaches the surface, surface runoff begins to form. The calculation of runoff generation is shown in Eq. (4):

$$R_3 = (i - f) \times \Delta t \tag{4}$$

where, R_3 indicates the runoff generation in the permeable area, the unit is mm; *i* indicates the rainfall intensity, the unit is mm/h; *f* indicates the infiltration rate, the unit is mm/h; Δt indicates the rainfall duration, the unit is h.

Therefore, under the same conditions, no runoff and impervious areas, sloping and impervious areas and permeable areas form runoff in sequence. Each sub-catchment area will perform runoff calculations according to different land surface types in the area. Then, they are weighted averaged to obtain the runoff process line of the sub-catchment.

2.2.4. Computation model of confluence

2.2.4.1. Surface confluence calculation The process of the surface confluence refers to the process of bringing together parts of the runoff into an exit section and rainwater pipe network [18,19]. The calculation of surface confluence uses a nonlinear reservoir model and is discharged into the river network. The schematic diagram of the nonlinear reservoir model is shown in Fig. 3.

The nonlinear reservoir model is obtained by solving the continuous equation and the Manning equation in parallel. The continuous equation is shown in Eq. (5):

$$\frac{dV}{dt}=A\frac{dd}{dt}=Ai^{*}-Q \tag{5}$$

where, V is the amount of surface water collected, $V = Ad$, the unit is m^3; d is the water depth, the unit is m; t represents time, the unit is s; A represents the surface area, the unit is m^2; i^* is the rainfall intensity in mm/S; Q is the outflow rate, the unit is m^3/s.

The outflow rate is calculated using the Manning equation, as shown in Eq. (6):

$$Q=\frac{1.49W}{n}(d-d_p)^{5/3}S^{1/2} \tag{6}$$

where, W is the sub-flow basin flow width, the unit is m; n is the surface Manning coefficient; d_p is the maximum surface depth of the surface, the unit is m; S is the average slope of the sub-basin.

The above two formulas are combined and merged into a nonlinear differential equation to solve the unknown d, as shown in Eq. (7):

$$\frac{dd}{dt}=i^{*}-\frac{1.49W}{An}(d-d_p)^{5/3}S^{1/2}=i^{*}+\mathrm{WCON}(d-d_p)^{5/3} \tag{7}$$

where, $WCON=-\frac{1.49W}{An}S^{1/2}$.

The above equation can be solved by the finite difference method. Therefore, the net inflow and net outflow on the right side of the equation can take the average of the time period, and the rainfall intensity i^* also takes the time period average, then the Eq. (7) can be simplified to the Eq. (8):

$$\frac{d_2-d_1}{\Delta t}=i\times\mathrm{WCON}\left[d_1-\frac{1}{2}(d_2-d_1)-d_p\right]^{5/3} \tag{8}$$

where, Δt denotes the time step, the unit is s; d_1 and d_2 respectively represent the initial value and the end time value of the water depth in the time period, and the unit is m.

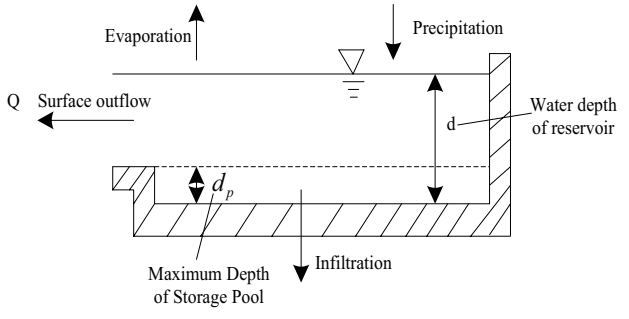

Fig. 3. Schematic diagram of the non-linear reservoir model.

Use Newton–Raphson to find the outflow Q during the period. (The Newton–Raphson iterative method solves d_2 of the above equations and finally substitutes d_2 into the Manning formula.)

2.2.4.2. Calculation of pipe network confluence For the calculation of pipe network confluence, the SWMM model provides three methods, namely constant flow method, motion wave method and dynamic wave method [20,21].

Constant flow method: The constant flow method is the simplest method of confluence calculation, which assumes that the flow of water is constant and uniform during each calculation period. This method cannot consider the change of accumulation, return, inlet and outlet losses, countercurrent and pressurized flow of the pipe, and is suitable for continuous long-term preliminary simulation.

Motion wave method: The motion wave method uses a continuous equation and a momentum equation to simulate the flow of water in each pipe segment. It assumes that the slope of the pipe is the same as the slope of the hydraulic line, and the maximum conveying flow of the pipe is calculated according to the Manning formula. The motion wave method can simulate the spatial and temporal changes of water flow in a pipe, but it still cannot account for return water, inlet and outlet losses, countercurrent and pressurized flow. It is only suitable for simulation calculations of the upstream of the drainage system and the portion of the dendrite network.

Dynamic wave method: Dynamic wave is the most complex and most accurate function calculation method by solving the complete Saint–Venant equations for confluence calculation. It can take into account the change of accumulation, return, inlet and outlet losses, countercurrent and pressurized flow of the canal. The dynamic wave method simulates an annular pipe channel system and a fork system with multiple downstream pipe segment nodes. This method is sensitive to the time step and must be calculated with a small-time step to ensure the accuracy of the calculation results.

2.2.4.3. Model verification After simulating the 2017 rainfall data, the surface runoff and flow calculus continuity errors were –0.22% and –0.02%, respectively, all within 10% of the model requirements. This shows that the simulated quality is very good, and there is a negligible quality balance continuity error for runoff and calculation. The simulation results can be used for further research and application.

2.3. Setting of simulation scenarios and LID measures

The parameters required for the model to run mainly include simulation options, rainfall conditions, and LID measures.

2.3.1. Setting of simulation options

It mainly includes common options, dates, time steps, dynamic waves, report settings, and files. Set the following parameters in the simulation profile: (1) *Simulation time and unit*: including simulation start date, simulation end date, simulation report start date, and report interval time is 1 min. (2) *Runoff*: The infiltration method uses the Horton model,

and the rainy season takes 1 min for a long time. (3) *Pipe network calculation parameters*: the pipe network confluence uses dynamic wave mode, and the pipe network calculation time step is 10 s. (4) *Simulation conditions*: Corresponding matching of rainfall conditions, such as once every 3 and 5 y.

2.3.2. Setting of rainfall scenarios

The main input parameters of rainfall data include rainfall data type, recording interval, and rainfall data time series [22,23]. Based on the study of the storm intensity formula in the study area, the return period is 1a, 3a, 5a, 10a, 20a, the rainfall duration is set to 120 min, and the rain peak coefficient is 0.385. Based on the SWMM model, the rainfall process of a specific scenario was synthesized to test the rain and flood confluence process in the study area. The designed rainstorm rainfall process lines in different recurrence periods are shown in Fig. 4.

2.3.3. Adjustment of LID facilities

The LID measure, as a property of a catchment area, is a low-impact development facility designed to capture surface runoff and combine retention, infiltration, and evaporation. The low-impact development and construction model is constructed, and the model is simulated and the program is repeatedly adjusted until the simulation result meets the control target value. The deployment of LID measures is mainly aimed at controlling the total amount of runoff in the study area. According to the characteristics of each facility of LID, the selected LID facilities include a green roof, permeable pavement, recessed green space and grass ditch. Refer to the values of the parameters provided in the SWMM model manual and the relevant literature reviewed to establish the parameters of the different unit layers of the LID facility [24]. Finally, the design values of the control indicators obtained in the study area are shown in Table 1.

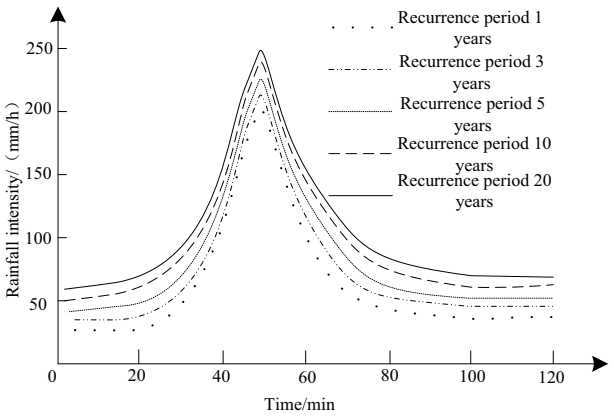

Fig. 4. Rainfall sequence diagram in the same reproduction period.

3. Results

3.1. Simulation results of the study area

The simulation results of surface runoff can reflect the influence of the type of underlying surface on the runoff in the study area. In theory, surface runoff refers to the amount of rainfall that is deducted from evaporation, surface water storage, and infiltration, and flows into the river through the ground and pipeline systems. The relationship between rainfall, infiltration and runoff in the study area under different return periods is shown in Table 2 during the method of managing the rainwater in the country park.

It can be seen from Table 2 that as the rainfall return period increases, the total rainfall, total infiltration, total runoff, surface water storage, and runoff coefficients gradually increase.

3.2. Impact of LID measures on runoff in the study area

In the model, it is assumed that the runoff treated by the LID facility will flow into the permeable zone in each sub-catchment area for further treatment. Using the low-impact development rainwater system model constructed above, the stormwater runoff in the study area was simulated when the total rainfall was 27.65 mm. The total amount of rainwater in the study area before and after the implementation of the LID facility was obtained to verify whether the target total discharges flow in the study area was zero when the designed rainfall was 27.65 mm. The simulation results are shown in Fig. 5.

From the above results, it is understood that the peak cut amount after the LID is performed is 21.16 m^3/s, and the total radial flow rate is 13.61 mm. The total stormwater discharge in the study area after LID implementation is always zero.

Besides, the rainfall-runoff changes after the implementation of the LID in the study area were simulated under different rainfall return period scenarios (including the 1a, 3a, 5a, 10a, 20a return period). The total emissions of the study area after the LID implementation were compared with the simulation results before the LID implementation to obtain the

Table 1
LID control indicators under different land-use types

Land use types		Roofing	Road	Greenland	Square	Total/km^2
Measure of area		1.54	1.11	1.66	0.08	4.39
Selection of control indicators for LID	Green roof	18%				0.27
	Permeable pavement		50%		42%	0.58
	Grassed swales			3%		0.03
	Concave green space			4%		0.05

Table 2
Surface runoff simulation results in the study area

Recurrence period	1*a*	3*a*	5*a*	10*a*	20*a*
Rainfall/mm	58.04	75.57	84.26	94.78	105.84
Total evaporation/mm	0	0	0	0	0
Total infiltration/mm	18.02	18.27	18.41	18.48	18.58
Total runoff/mm	32.04	46.98	54.71	64.15	74.24
Surface water storage/mm	8.01	10.34	11.17	12.17	13.04

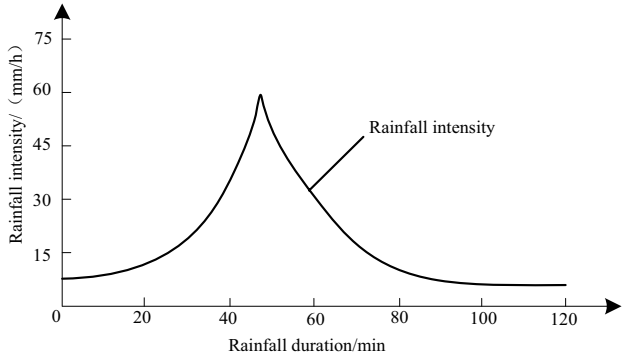

(a)

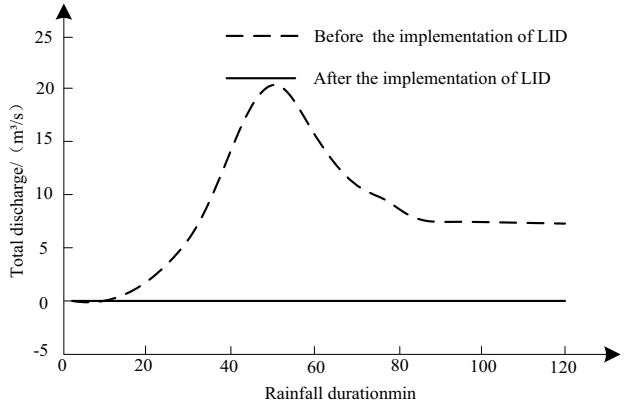

(b)

Fig. 5. Simulation results of rainfall and total emissions. (a) Rainfall intensity and (b) Comparison of total emissions before and after LID implementation.

simulation results before and after the LID implementation under five different reproduction periods. It can be seen from the simulation results that under the regulation of LID, the rainfall infiltration in the study area increased by 20.08, 26.66, 29.7, 33.25, and 36.78 mm in different return periods, and the total rainfall runoff was reduced. The rates were 86%, 75%, 71%, 67%, and 63%, respectively, and the reduction rates for flood peak flow were 87%, 76%, 68%, 61%, and 54%, respectively. The peak traffic occurrence time is 7–13 min before the LID implementation. As the rainfall intensity increases, the LID measures gradually reduce the total amount of surface runoff and peak runoff in the study area.

3.3. Simulation results and analysis of pipeline node overflow

In the study area, the simulation results of the overloaded pipeline and overflow nodes before and after LID regulation are shown in Table 3.

According to the simulation results, when the rainfall return period $P = 1a$, a total of 15 nodes overflow. At this time, there was a slight water accumulation in the study area, and the degree of internal hemorrhage was light. When the rainfall return period $P = 3a$, $5a$, $10a$, $20a$, the number of nodes overflowing in the study area gradually increased, which were 20, 22, 24, and 28 respectively. The cumulative overflow time, the longest overflow time and the total amount of overflow also increase. However, under the control of LID, the ground runoff coefficient of the study area has decreased, and the runoff in the pipe network system has also decreased, and the flow rate and node flow of each pipe section of the pipeline have been significantly reduced. These alleviate the drainage pressure of the drainage network system.

3.4. Design and distribution of stormwater management in the study area

Based on the SWMM and the implementation of LID measures, the stormwater management program for the country parks in the study area was designed. The overall distribution of stormwater management design in the study area is shown in Fig. 6.

3.4.1. Duplex planting and sunken green space

It is necessary to increase the planting density and variety of plants. Through the layer block of plants, the rainwater runoff reduces the erosion of the mountain and increases the penetration of rainwater. Based on existing vegetation, the configuration of trees, shrubs and ground cover plants is increased, and multiple planting is carried out to enrich the level of vegetation. Large-scale greening is carried out in areas with large exposed areas of the mountain. The fish scale holes and horizontal steps are combined with the terrain to intercept the rainwater, forming a sunken green space to purify and infiltrate the rainwater. The main selection of planting trees is Huang Hu, Wu Jiao Feng, Guo Yu, Chestnut, White Wax, etc. The shrubs are mountain peach, clove, pearl plum, eucalyptus, gold and silver wood, etc.; the ground cover is Euonymus, Fufangteng, Yingchun, Forsythia and so on. The designed area of the sinking green space is about 18.5 hectares, the water storage depth is 100–150 mm, and the total designed water storage is about 15,385 m^3, as shown in the green area in Fig. 6.

Table 3
Comparison of simulation results of overflow nodes and overload pipelines in the study area before and after LID regulation

Recurrence period		1*a*		3*a*		5*a*		10*a*		20*a*	
Measures		No LID regulation	LID regulation	No LID regulation	LID regulation	No LID regulation	LID regulation	No LID regulation	LID regulation	No LID regulation	LID regulation
Overflow node	Number of overflow nodes/numbers	15	0	20	5	22	8	24	13	28	15
	Total overflow/1,000 m^3	6.93	0	11.3	1.02	15.6	2.35	16.6	4.8	19.5	8.4
Overload pipeline	Section of overloaded pipelines/number	51	10	66	22	69	29	73	39	81	43
	Full pipe rate/%	30	6	39	13	41	17	43	23	48	25
	Average full flow time/min	36	12	43	28	48	32	54	34	56	39

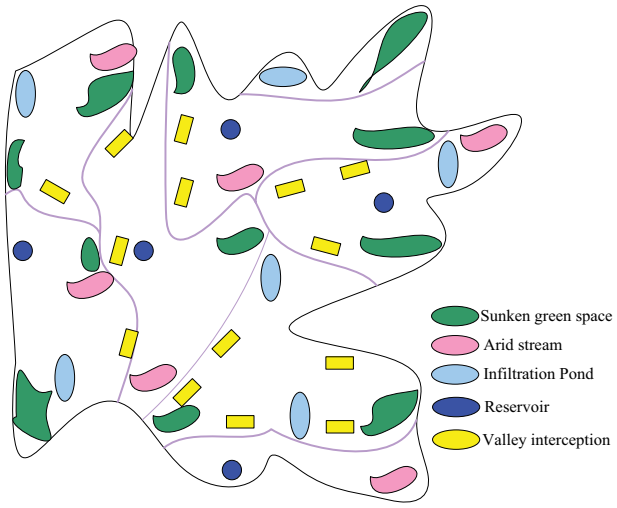

Fig. 6. Overall distribution of rainfall flood management design in the research area.

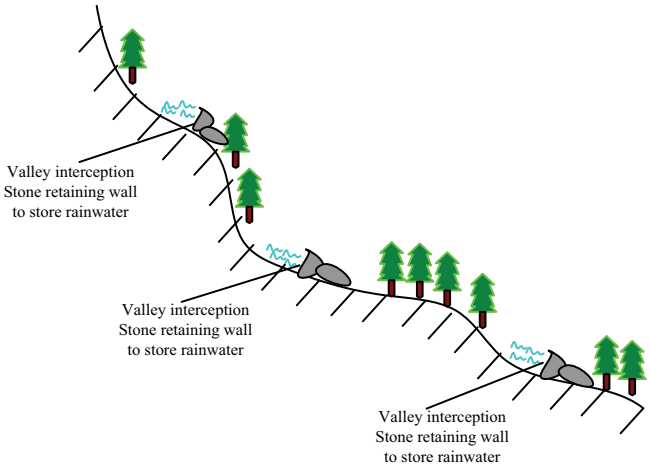

Fig. 7. Valley interception profile.

3.4.2. Drought river

Combined with the terrain of the study area and the confluence of rainwater confluence, the natural design drought rive landscape is designed according to local conditions. The use of vegetation, rocks, and soil to filter and block stormwater runoff not only reduces surface erosion and soil erosion but also creates the natural stream landscape. Drought river's design has a total storage capacity of 528 m^3, as shown in the pink area in Fig. 6.

3.4.3. Permeation ponds and reservoirs

The permeation ponds and reservoirs are designed in areas with large catchment, which can regulate the rainwater of the mountain, and have the effect of reducing the peak flow of rainwater and collecting rainwater for reuse. The total designed water storage is 1,762 m^3, as shown in the dark blue and light blue areas in Fig. 6.

3.4.4. Valley water storage facilities

In complex orogenic belts, there are 29 large catchment valleys. To weaken the erosion of the valley by the rainwater runoff, combined with the mountain terrain for the design of the rainwater interception facility, the valley interception profile is shown in Fig. 7. Due to the large slope of the valley, the amount of rainwater confluence is large. In the valley, multiple layers of rainwater interception facilities are arranged according to the terrain to block rainwater, such as horizontal steps and fish-scale pits. At the time of design, we should try our best to meet the needs of the landscape and realize its practicality and aesthetics of the landscape. Combined with the existing landscape, some designs can form the stacked landscape with the characteristics of the mountain park during the rainy season. The total design storage capacity of

the valley storage facility is expected to be 6,067 m^3, as shown in the yellow area in Fig. 6.

3.5. Calculation of water storage

The design results of the water storage capacity of the country parks in the study area are shown in Table 4.

It is calculated that the total designed water storage of stormwater management in the country park of the study area is about 23,742 m^3, which is about 1,227.58 m^3 more than the standard theoretical water storage. This achieved the desired results and completed the goal of stormwater management in the country parks of the study area.

4. Discussion

In this paper, the SWMM model for stormwater management of the country parks in the complex orogenic belts in the study area can accurately simulate the surface runoff in different return periods. As shown in the surface runoff simulation results of the study area in Table 3, when the return period is $P > 1a$, the infiltration amount basically reaches a saturation state. It can be seen from the simulation results of five different rain conditions that rainfall is a direct influencing factor of runoff, and the change of runoff shows a strong correlation with the change of rainfall. Under the above five rainfall conditions, the peak runoff of the system is 42.19, 54.35, 60.42, 67.87 and 73.99 m^3/s, respectively.

After the implementation of stormwater management in the country park based on LID measures, the study area can reach the target of an 80% runoff control rate. That is to say, when the designed rainfall is 27.65 mm, the rainwater in the study area is not discharged, as shown in Fig. 5. The LID measures can effectively reduce the runoff of 63%–86% and alleviate the drainage pressure of the drainage network, improve the design standard of the rainwater pipeline in the study area, and reduce the risk of intrinsic risk in the study area, as shown in Table 4. The reason is that low-impact development measures are mainly by changing the proportion of impervious areas on the underlying surface and the way of rainwater runoff [25–28]. It reduces runoff discharge through the effects of soil and vegetation retention, infiltration, filtration, etc., and reduces the total runoff and peak flow in the study area. It also delays the occurrence of peak runoff and increases the ability of the study area to absorb rainwater [29,30].

According to the analysis of the status quo of the country parks in complex orogenic belts based on the SWMM model and the stormwater management based on the LID measures, the actual stormwater management planning for the country parks in the study area is carried out. Apply the research theory to the design practice, and appropriately apply the landscaped facilities such as double planting and sinking green space, durable rive, seepage pond, reservoir, and valley storage facility to play the functions of rainwater transmission, infiltration, and savings. The design area of the country park in the study area can reach a total of 23,742 m^3. Based on perfecting the landscape facilities, it achieves the goal of rational use of rainwater and alleviates the water ecological problems in complex orogenic belts.

Table 4
Result of design storage of rainfall and flood management in country parks

Design of rainfall flood management	Storage depth (m)	Designed storage capacity (m^3)
Sunken green space	0.11–0.16	15,385
Arid stream	0.55	528
Infiltration pond and storage pond	–	1,762
Valley storage facilities	0.55	6,067
Total		23,742

5. Conclusions

Combining complex orogenic belts' country parks with stormwater management plays a good role in improving the environment and increasing the social value of complex orogenic belts. A country park in complex orogenic belts in the south of J City is used as a research area. The SWMM (stormwater management model) is established based on the rainfall data, and the LID module is used for stormwater management. The results of the study are as follows:

- There is a strong correlation between runoff and rainfall. The greater the rainfall intensity is, the greater the runoff is. There is a certain time difference between the peak of rainfall and the peak of runoff. The occurrence time of the runoff peak in the region studied in this paper is about 50 min, and it lags behind the peak of rainfall for about 6 min.
- The regulation of LID reduces the ground runoff coefficient of the study area, and the runoff into the pipe network system also decreases. The flow rate and node flow of each pipe section of the pipeline are significantly reduced. That alleviates the drainage pressure of the drainage pipe network system.
- The water storage capacity of the compound planting and sinking green space, the durable rive, the infiltration pond, and the reservoir, and the valley storage facility designed by stormwater management in the study area are 15,385; 528; 1,762; and 6,067 m^3, respectively. The total water storage capacity can reach 23,742 m^3, which can realize the rational use of rainwater.

References

[1] Y.M. Wu, S.K. Chen, T.C. Huang, Relationship between earthquake *B*-values and crustal stresses in a young orogenic belt, Geophys. Res. Lett., 45 (2018) 1832–1837.
[2] B.X. Mao, Two methods for sliding mode synchronization of fractional-order newton-Leipnik chaotic systems, J. Jilin Univ. (Sci. Ed.), 56 (2018) 708–712.
[3] X. Xing, Y. Wang, P.A. Cawood, Early Paleozoic accretionary orogenesis along Northern margin of Gondwana constrained by high-Mg metaigneous rocks, SW Yunnan, Int. J. Earth Sci., 106 (2017) 1469–1486.
[4] G. Balestro, A. Festa, A. Borghi, Role of late Jurassic intra-oceanic structural inheritance in the Alpine tectonic evolution of the Monviso meta-ophiolite complex (Western Alps), Geol. Mag., 155 (2017) 233–249.
[5] Z.J. Lu, X. Liu, Y.G. Qin, An adaptive multi-sensor management method for cooperative perception, J. China Acad. Electron. Inf. Technol., 12 (2017) 353–358.

[6] C. Yang, C. Wei, Ultrahigh temperature (UHT) mafic granulites in the East Hebei, North China Craton: constraints from a comparison between temperatures derived from REE-based thermometers and major element-based thermometers, Gondwana Res., 46 (2017) 156–169.
[7] Z. Liu, W. Peng, M. Motahari-Nezhad, Circulating fluidized bed gasification of biomass for flexible end-use of syngas: a micro and nanoscale study for production of bio-methanol, J. Cleaner Prod., 129 (2016) 249–255.
[8] H. Wang, H. Zhong, G. Bo, Existing forms and changes of nitrogen inside of horizontal subsurface constructed wetlands, Environ. Sci. Pollut. Res., 25 (2018) 771–781.
[9] K. Sarkarinejad, Z. Heibati, Vorticity analysis in the Zagros orogen, Shiraz area, Iran, Int. J. Earth Sci., 106 (2017) 1–25.
[10] W.J. Tan, Y.D. Chen, L. Yang, Energy coordinated control method for DC microgrid with photovoltaic, J. Power Supply, 16 (2018) 76–85.
[11] H. Mvondo, D. Lentz, M. Bardoux, Metamorphism in Neoarchean granite-greenstone belts: insights from the link between Elu and Hope Bay belts (~2.7 Ga), Northeastern Slave Craton, J. Geol., 125 (2017) 203–221.
[12] B. Guo, S. Liu, C. Xu, K-rich granitoid magmatism at the Archean–Proterozoic transition in Southern Jilin: insights into the Neoarchean crustal evolution of the Northeastern part of the North China Craton, Gondwana Res., 58 (2018) 87–104.
[13] G.I. Alsop, R. Weinberger, S. Marco, Distinguishing thrust sequences in gravity-driven fold and thrust belts, J. Struct. Geol., 109 (2018) 99–119.
[14] S. Madhav, A. Ahamad, A. Kumar, Geochemical assessment of groundwater quality for its suitability for drinking and irrigation purpose in rural areas of Sant Ravidas Nagar (Bhadohi), Uttar Pradesh, Geol. Ecol. Landscapes, 2 (2018) 127–136.
[15] T.F. Zhang, Power management of a new generation navigation satellite, Chin. J. Power Sources, 41 (2017) 1055–1056.
[16] L. Kai, J. Zhang, S.A. Wilde, U-Pb dating and Lu-Hf isotopes of detrital zircons from the Southern Sikhote-Alin orogenic belt, Russian Far East: tectonic implications for the early cretaceous evolution of the Northwest Pacific Margin, Tectonics, 36 (2017) 2555–2598.
[17] R. Grandin, M.P. Doin, L. Bollinger, Long-term growth of the Himalaya inferred from interseismic InSAR measurement, Geology, 40 (2017) 1059–1062.
[18] F. Kohanpour, W. Gorczyk, M.D. Lindsay, Examining tectonic scenarios using geodynamic numerical modeling: Halls Creek orogen, Australia, Gondwana Res., 46 (2017) 95–113.
[19] M. Kamal, R. Younas, M. Zaheer, M. Shahid, Treatment of municipal wastewater through adsorption using different waste biomass as activated carbon, J. Clean Was, 3 (2019) 21–27.
[20] A. Rezaei, H. Hassani, S.B.F. Mousavi, N. Jabbari, Evaluation of heavy metals concentration in Jajarm bauxite deposit in Northeast of Iran using environmental pollution indices, Malaysian J. Geosci., 3 (2019) 12–20.
[21] D.P. Zhang, P.L. Xu, L.Q. Ge, Research on quality assessment of elevator maintenance based on virtual technology, Autom. Instrum., 231 (2019) 36–38.
[22] X. Wang, J.S. Li, S.M. Li, Study on the interception effects of an ecological pond on nitrogen and phosphorus in the rainfall-runoff of rice field, J. Hydraul. Eng., 48 (2017) 291–298.
[23] A.J. Ahamed, K. Loganathan, Water quality concern in the Amaravathi River Basin of Karur district: a view at heavy metal concentration and their interrelationships using geostatistical and multivariate analysis, Geol. Ecol. Landscapes, 1 (2017) 19–36.
[24] X. Zhang, High-speed information network security management simulation method research, Comput. Simul., 34 (2017) 284–287.
[25] R.M. Fuentes Rivas, G. Santacruz De Leon, J.A. Ramos Leal, Characterization of dissolved organic matter in an agricultural wastewater-irrigated soil, in semi-arid Mexico, Rev. Int. De Contam. Ambiental, 33 (2017) 575–590.
[26] H.J. Blaauw, Global warming: sun and water, Energy Environ., 28 (2017) 468–483.
[27] K. Khanchoul, S. Boubehziz, Spatial variability of soil erodibility at El Hammam catchment, Northeast of Algeria, Environ. Ecosyst. Sci., 3 (2019) 17–25.
[28] P. Almasi, S. Soltani, Assessment of the climate change impacts on flood frequency (case study: Bazoft Basin, Iran), Stochastic Environ. Res. Risk Assess., 31 (2017) 1171–1182.
[29] M.T. Sarwar, Z.H. Hui, Y.J. Xin, S.W. Jiang, T. Yong, L.B. Jie, T.S. Song, Mitigation techniques to overcome water scarcity issues, Water Conserv. Manage., 3 (2019) 30–31.
[30] S. Yousefi, S. Mirzaee, S. Keesstra, Effects of an extreme flood on river morphology (case study: Karoon River, Iran), Geomorphology, 304 (2018) 30–39.